Chapter 12
The Structure, Function and Roles of the Archaeal ESCRT Apparatus

Rachel Y. Samson, Megan J. Dobro, Grant J. Jensen, and Stephen D. Bell

Abstract Although morphologically resembling bacteria, archaea constitute a distinct domain of life with a closer affiliation to eukaryotes than to bacteria. This similarity is seen in the machineries for a number of essential cellular processes, including DNA replication and gene transcription. Perhaps surprisingly, given their prokaryotic morphology, some archaea also possess a core cell division apparatus that is related to that involved in the final stages of membrane abscission in vertebrate cells, the ESCRT machinery.

Keywords ESCRT-III • Vps4 • cdvA • cdvB • Cytokinetic ring • Archaeal cell constriction • *Sulfolobus acidocaldarius* • AAA+ protein • MIT domain • Electron cryotomography • Cryo-ET • STIV

R.Y. Samson
Department of Molecular and Cellular Biochemistry, Indiana University, Simon Hall MSB, 212 S Hawthorne Drive, Bloomington, IN 47405, USA
e-mail: rsamson@umail.iu.edu

M.J. Dobro
School of Natural Science, Hampshire College, Amherst, MA 01002, USA

G.J. Jensen
Division of Biology, California Institute of Technology, Pasadena, CA 91125, USA

Howard Hughes Medical Institute, California Institute of Technology, Pasadena, CA 91125, USA
e-mail: jensen@caltech.edu

S.D. Bell (✉)
Department of Molecular and Cellular Biochemistry, Indiana University, Simon Hall MSB, 212 S Hawthorne Drive, Bloomington, IN 47405, USA

Department of Biology, Indiana University, Simon Hall MSB, 212 S Hawthorne Drive, Bloomington, IN 47405, USA
e-mail: stedbell@indiana.edu; sdbell123@gmail.com

© Springer International Publishing AG 2017

J. Löwe, L.A. Amos (eds.), *Prokaryotic Cytoskeletons*, Subcellular Biochemistry 84, DOI 10.1007/978-3-319-53047-5_12

The Diversity of Archaea

Since their discovery in the late 1970's by Carl Woese, it has become apparent that archaea are abundant components of the biosphere (Woese and Fox 1977). Archaea have been isolated from a huge diversity of ecological niches, ranging from Antarctic surface waters to hydrothermal vent systems, where the organisms grow at temperatures in excess of 100 °C. Although the extremophilic archaea are probably the best known, there are many archaeal species adapted to mesophilic environments. By way of example, ammonia-oxidizing archaea are abundant in soil samples and the human microbiome is populated by a number of archaeal species, most notably the gut methanogen *Methanobrevibacter smithii* (Stahl and de la Torre 2012; Bang and Schmitz 2015). Although no archaeal pathogens have yet been described, there are examples of archaeal-bacterial consortia, archaea existing in symbiosis with marine sponges and there have been some links proposed between archaeal abundance and human health (Bang and Schmitz 2015; Schink 1997; Preston et al. 1996).

With the ever-increasing taxonomic sampling of archaea, phylogenetic analyses have revealed that the archaeal domain of life can be split into two main groupings or "super-phyla" – the Euryarchaea and the "TACK" superphylum (Guy and Ettema 2011). TACK comprises the Thaumarchaea, Aigarchaea, Crenarchaea and Korarchaea and has been proposed to be the closest grouping of archaea to the last common ancestor between Archaea and Eukaryotes (Guy and Ettema 2011). Indeed, recent work from Embley and colleagues has suggested that the divergence of Archaea and Eukaryotes occurred following the emergence of the Euryarchaeal lineage (Williams et al. 2013). This proposal has profound implications for the evolution of life on Earth, not least of which is the revelation that there are two, not three, domains of life (Fig. 12.1).

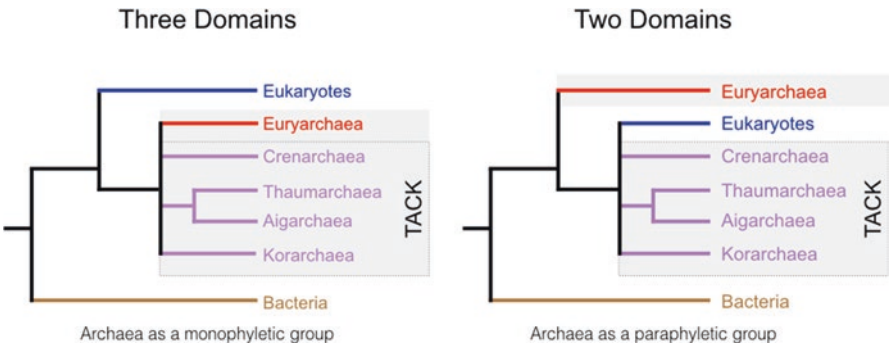

Fig. 12.1 Alternative phylogenetic trees for the evolution of cellular organisms. The *left* hand image shows the classical tree proposed by Carl Woese revealing three domains of life. The *right*-hand phylogenetic tree illustrates the recent proposal by Embley and colleagues that eukaryotes arose from within the archaeal lineage, following the divergence of the Euryarchaea. This topology is compatible with earlier proposals from the Lake laboratory (Rivera and Lake 2004; Williams et al. 2013; Woese and Fox 1977)

Interestingly, examination of the limited data available on archaeal chromosome copy number and cell-cycle organization provides hints that these processes within TACK organisms bear closer resemblance to eukaryotes than do their counterparts in euryarchaea (Samson and Bell 2011). More specifically, TACK organisms have defined gap phases between DNA synthesis and cell division (Samson and Bell 2011, 2014; Bernander 1998). Indeed, the eukaryotic cell cycle nomenclature of G1, S, G2 and M phase is commonly applied to archaeal cell cycle parameters. However, it is important to emphasize that, at the mechanistic level, archaeal M-phase is completely unrelated to eukaryotic mitosis. In contrast to the defined cell cycle phases seen in TACK species, the limited number of euryarchaea that have been studied reveal less obvious partitioning of the cell cycle. In fact, it appears that some species may have overlapping DNA replication and cell division phases. In agreement with this latter proposition, the members of the Euryarchaea generally have high chromosome copy numbers. For example, *Haloferax volcanii* has about 15 copies of its chromosome during exponential growth (Zerulla and Soppa 2014; Breuert et al. 2006). The polyploidy of euryarchaea contrasts with the TACK superphylum organisms that have been characterized, all of which show a simple one to two chromosome copy number oscillation during their cell cycle (Lundgren et al. 2008). Furthermore, studies of the crenarchaeon *Sulfolobus solfataricus* provided evidence for cohesion of sister chromatids following the completion of DNA replication (Robinson et al. 2007). Thus, at both phylogenetic and organizational levels, members of the TACK superphylum show remarkable similarities to eukaryotes.

Cell Division Machineries

Initial studies published in 1996 of the euryarchaea *Halobacterium salinarum* and *Pyrococcus woesei* by the Jackson and Margolin labs, respectively, identified archaeal homologs of the central, and near universal, bacterial cell division protein FtsZ (Margolin et al. 1996; Baumann and Jackson 1996). Subsequently, the Lutkenhaus laboratory revealed that the *Haloferax volcanii* FtsZ formed a ring-like structure at mid-cell, coincident with the site of membrane constriction during cell division (Wang and Lutkenhaus 1996). As complete archaeal genome sequences became available, all of euryarchaea initially, further FtsZ homologs were identified, revealing that this protein was found in many archaea as well as bacteria. Subsequent landmark structural studies by Lowe and Amos revealed the first crystal structure of FtsZ – using the protein from the euryarchaeon *Methanocaldococcus jannaschii* (Lowe and Amos 1998).

However, the apparent ubiquity of archaeal FtsZ was challenged by an analysis from the Doolittle laboratory of the first complete crenarchaeal genome, that of *Aeropyrum pernix*, in which it was recognized that there was no identifiable homolog of FtsZ (Faguy and Doolittle 1999; Kawarabayasi et al. 1999). The absence of FtsZ in other crenarchaea was confirmed with the elucidation of the genome sequences of *Pyrobaculum aerophilum*, and *Sulfolobus tokodaii* and *Sulfolobus*

solfataricus (Fitz-Gibbon et al. 2002; She et al. 2001; Kawarabayasi et al. 2001). As detailed elsewhere in this book, an actin homolog, termed crenactin, was identified in *Pyrobaculum* and other members of the Thermoproteales (Yutin et al. 2009). Immunolocalization studies of crenactin were described as showing helical-like structures within the rod-shaped *Pyrobaculum* cells (Ettema et al. 2011). These structures were interpreted as providing evidence for a cytoskeletal role for the crenactin. However, studies of bacterial MreB provide a cautionary note for this interpretation. Initial work suggested that MreB formed a coherent helical cytoskeleton in rod-shaped bacteria (Jones et al. 2001). Immunolocalization and use of fluorescently tagged proteins supported this conclusion. More recently, however, it has been proposed that the helical structures may have arisen as a consequence of appending a fluorescent tag to the MreB protein (Swulius and Jensen 2012). Further, additional studies have led to the proposal that MreB forms dynamic circumferential bands around the cell, perpendicular to the long axis, and appears to play a key role in cell wall biosynthesis (Errington 2015; Garner et al. 2011; Dominguez-Escobar et al. 2011). With respect to the archaeal actin homolog, the current limited and low-resolution data derived from analyses of fixed cells cannot exclude the possibility that crenactin might play an analogous role in S-layer synthesis in the rod-shaped Thermoproteales. Despite the completion of the *Sulfolobus solfataricus* genome in 2001, it would be a further 6 years before candidates for the *Sulfolobus* cell division machinery were identified. Figure 12.2 summarizes the distribution of potential cytoskeletal and cell division proteins across the archaeal domain of life (Makarova et al. 2010).

ESCRT Proteins

In 2007, the laboratory of Roger Williams at the LMB in Cambridge, studying the eukaryotic ESCRT (**E**ndosomal **S**orting **C**omplex **R**equired for **T**ransport) apparatus, identified a *Sulfolobus* homolog of the ESCRT system component, Vps4. Their work revealed a striking structural relationship between the so-called MIT domain of the archaeal Vps4 with its counterpart in yeast Vps4 (Obita et al. 2007). Furthermore, they identified *Sulfolobus* homologs of the eukaryotic ESCRT-III proteins. As that initial study used the eukaryotic names for the archaeal homologs, we will retain that convention in this chapter. The eukaryotic ESCRT machinery has been comprehensively dissected at the molecular level and there are a number of excellent reviews that describe that work (Hurley 2015; Henne et al. 2013; McCullough et al. 2013). Accordingly, we will give an extremely brief and simplistic summary of the roles of ESCRT in eukaryotes.

First identified by virtue of its role in endosome sorting, the ESCRT pathway directs the invagination and scission of membranes. A series of elegant *in vitro* reconstitution studies revealed that the ESCRT-III proteins form filaments and are

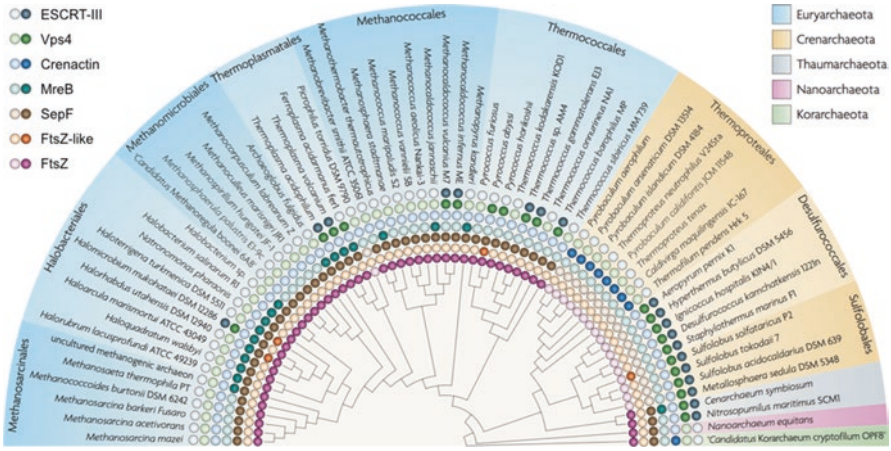

Fig. 12.2 Distribution of candidate cytoskeletal and cell division proteins across the archaeal domain of life (Figure taken from Makarova et al. 2010 with permission). Filled-in *circles* indicate the presence of one or more genes encoding homologs of the indicated proteins

necessary and sufficient to drive membrane constriction and scission in a system reconstituted with giant unilameller vesicles. Vps4 is an AAA+ ATPase that can interact with ESCRT-III, (see below for details). Dependent on its ability to hydrolyze ATP, Vps4 facilitates depolymerization and subsequent recycling of ESCRT-III to membranes. Delivery of ESCRT-III to its site of action in endosomal sorting is dependent on the sequential assembly of a protein scaffold composed of the ESCRT-0, ESCRT-I and ESCRT-II complexes. With the exception of one lineage, whose existence is inferred solely from metagenomic studies (Spang et al. 2015), these earlier ESCRT-III recruiting complexes are absent from archaea.

Following the discovery of ESCRT's role in trafficking, subsequent studies have revealed that this apparatus plays pivotal roles in a number of other processes that involve membrane scission events. These include viral egress from infected cells, plasma membrane wound healing, nuclear membrane reformation following chromosome segregation and membrane abscission – the final stage of cytokinesis in metazoan cells (Hurley 2015).

The Sulfolobus *ESCRT Machinery*

In 2008, work by our laboratory (RYS and SDB) in collaboration with the Williams lab and an independent study by Bernander and colleagues provided evidence that the *Sulfolobus* ESCRT machinery played a role in archaeal cell division (Samson et al. 2008; Lindas et al. 2008).

In *Sulfolobus*, the *vps4* gene is encoded adjacent to a gene for an ESCRT-III protein. An additional gene, called *cdvA*, is found immediately upstream of this

operon (Fig. 12.3). As discussed below, *cdvA* is a distinct transcription unit from ESCRT-III and Vps4 genes (Samson et al. 2011; Wurtzel et al. 2010).

Sulfolobus possesses three other ESCRT-III genes. The four ESCRT-III paralogs are variable in length, with the gene beside *vps4* encoding the longest open-reading frame. In addition to the core ESCRT-III α-helix-rich fold, this protein possesses a signature C-terminal winged-helix-like (wH-like) domain that is not found in the remaining paralogs (Fig. 12.3). A recent genetic study revealed that it was possible to individually delete the genes for the three shorter ESCRT-III paralogs and retain cell viability, albeit with reduced growth rate. In contrast, it was not possible to delete the gene for the wH domain-containing ESCRT-III protein, suggesting this protein is essential for viability (Yang and Driessen 2014).

Studies using synchronized *Sulfolobus acidocaldarius* cells revealed that transcripts for *vps4* and its proximal ESCRT-III gene, which are expressed as a bicistronic transcript, and the other orphan genes for the shorter ESCRT-III paralogs are maximally abundant in populations enriched with cells undergoing division (Samson et al. 2008). Similarly, the *cdvA* gene transcript showed cell cycle regulation, although its levels peaked slightly before those for ESCRT-III and Vps4 (Samson et al. 2011).

As well as being cell cycle regulated, transcript levels of the genes for CdvA, ESCRT-III and Vps4 are modulated in response to a number of insults to the cell, including UV-induced DNA damage, oxidative stress caused by hydrogen peroxide, viral infection and respiratory arrest caused by acetic acid treatment (Lindas et al. 2008; Ortmann et al. 2008; Maaty et al. 2009; Gotz et al. 2007; Frols et al. 2007).

The timing of expression of the *Sulfolobus* ESCRT components is compatible with a role in cell division. Immunolocalization studies on fixed cells revealed that polyclonal antisera raised against the wH-containing ESCRT-III and Vps4 localized

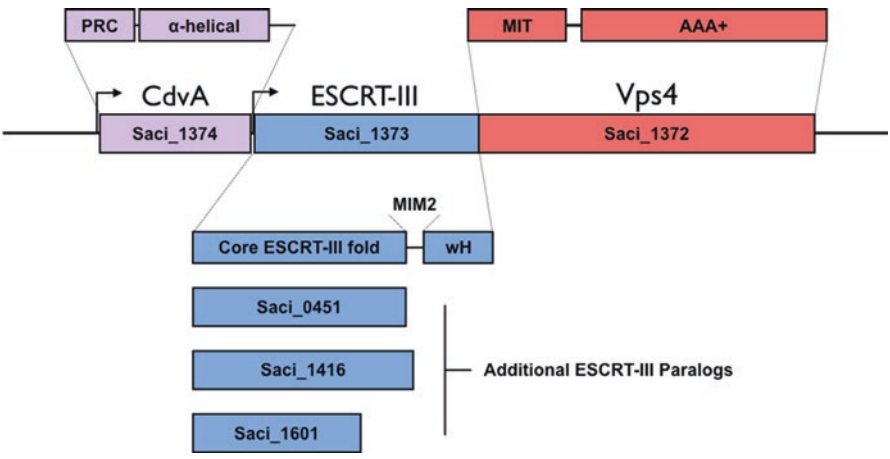

Fig. 12.3 The organization of the genes for the *Sulfolobus acidocaldarius* ESCRT-associated proteins. Principal domains of the encoded proteins are indicated. The Saci_XXXX names are from the original genome annotation (Chen et al. 2005)

to a belt between segregated nucleoids (Lindas et al. 2008; Samson et al. 2008). Furthermore, the location of the belt correlated with the site of membrane ingression in cells undergoing division. Dividing cells are very rare within asynchronous *Sulfolobus* populations, suggesting that cell division is a very rapid event. Similarly, very few cells are observed with segregated nucleoids, again suggesting that the process of chromosome segregation, the mechanism of which is entirely mysterious, is rapid and closely linked to the membrane ingression event. We note, however, that cells can be observed that have segregated nucleoids and contiguous ESCRT-III bands, and yet have no visible ingression of the membrane (Samson et al. 2008; Lindas et al. 2008). Thus, our working hypothesis is that nucleoid segregation occurs prior to ESCRT-III assembly.

A causal role for the *Sulfolobus* ESCRT system in cell division was supported by the conditional expression of a *trans*-dominant negative allele of *vps4* in *Sulfolobus solfataricus* cells (Samson et al. 2008). This allele, encoding an alanine substitution of the conserved glutamic acid residue in the so-called Walker B motif, allows ATP binding but prevents its hydrolysis. Previous work in mammalian cells revealed that expression of this and other ATPase-defective alleles impacts negatively on cell division (Carlton and Martin-Serrano 2007; Morita et al. 2007). Upon expression of this form of the protein in *Sulfolobus*, bloated cells up to four-times the usual diameter and with elevated DNA content were observed. In addition, abundant small membranous structures that lacked discernable DNA content were seen. The generation of these bloated cells and ghosts is compatible with impaired cell division processes (Samson et al. 2008).

In eukaryotes, the ESCRT-III proteins bind directly to membranes but are recruited to their sites of actions by the prior assembly of ESCRT-I and ESCRT-II complexes (Wollert and Hurley 2010). In contrast, we have been unable to detect direct membrane interaction by the *Sulfolobus* ESCRT-III proteins. Indeed, they lack the charged patch that has been shown to be important for membrane interaction by the eukaryotic proteins (Samson et al. 2011). Further, as discussed above, *Sulfolobus* lacks discernable homologs of the earlier ESCRT components.

The close linkage of the *cdvA* gene and its cell cycle regulated expression profile suggested it could be an early assembling component of the cell division machinery. In agreement with this, like ESCRT-III and Vps4, CdvA forms a ring-like structure at mid-cell that shrinks concomitant with division plane ingression. Intriguingly, mRNA levels for CdvA peak before those for ESCRT-III and Vps4, and CdvA structures can be detected prior to nucleoid segregation. Co-immunolocalization studies of late G2/early M-phase cells revealed that only a subset with CdvA structures were decorated with punctate foci of ESCRT-III. In contrast it was not possible to detect cells that were CdvA negative but ESCRT-III positive. In agreement with these observations, *in vitro* binding assays demonstrated that, while ESCRT-III was unable to bind directly to purified membranes, CdvA could. Futhermore, CdvA was capable of recruiting ESCRT-III to liposomes with consequential deformation of the membrane. Thus, taken together, these data indicate that CdvA forms a ring-like structure at mid-cell and serves as a platform for the subsequent recruitment of the ESCRT-III proteins (Samson et al. 2011).

Structures of Archaeal ESCRT Proteins

Structural studies of the ESCRT-machinery in eukaryotes and archaea have been aided by the strikingly modular nature of the proteins. As described below, this has allowed minimal interaction domains to be dissected and some highly informative structures of these domains with their partner peptides have been elucidated (Samson et al. 2008, 2011). In addition, the structures of the ATPase domain of Vps4 from *Sulfolobus solfataricus* (Sso) and *Acidianus hospitalis* (both crenarchaea of the order Sulfolobales) have been determined by the Sundquist lab using X-ray crystallography (Monroe et al. 2014) (Fig. 12.4).

Sso Vps4 is a 372 amino acid protein; the first 75 residues constitute a MIT domain, the structure of which was solved by the Williams laboratory (Obita et al. 2007). The MIT domain is separated from the AAA+ ATPase domain by a short and apparently flexible linker. As with many AAA+ proteins, Vps4 forms homo-oligomers and the Sundquist laboratory revealed Sso Vps4 forms a homohexamer in the presence of ATP or ADP following heat treatment (Monroe et al. 2014). The Sso Vps4 AAA+ domain structure does not reveal how the protein forms hexamers but modeling based on superimposition of the Sso Vps4 monomer on the AAA+ domain of P97 allowed a model to be built. The model was verified by mutation of predicted interfacial residues, resulting in a destabilization of the hexamer and consequential reduction in ATPase activity. As with many other AAA+ proteins, the ATPase active site lies at the interface between two protomers, with residues from both subunits

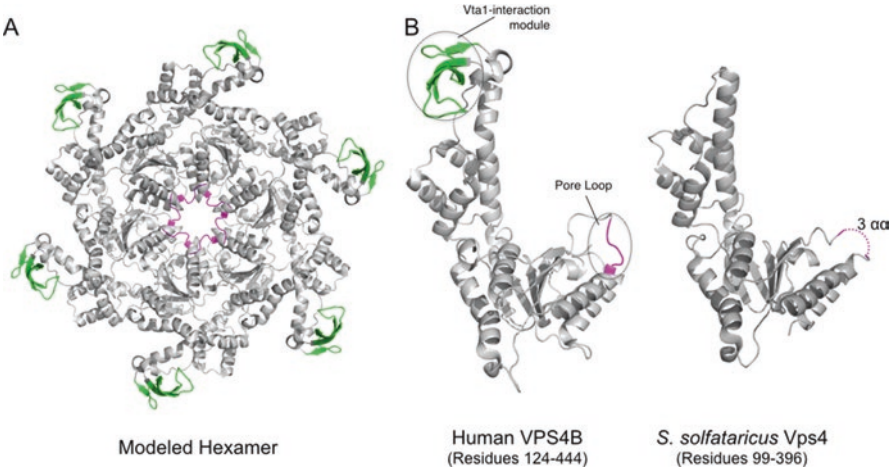

Fig. 12.4 (**a**) A modeled hexamer of human VPS4. The model was generated by superposition of the VPS4B monomer structure (PDB 1XWI) onto the symmetric hexamer structure of ClpX (PDB 4I9K). Pore loop 1 and the eukaryotic-specific Vta1 interaction module are colored magenta and green respectively (**b**) Comparison of monomers of human and *Sulfolobus* Vps4 (PDB 4LGM). 3 residues in the pore loop (*magenta*) of *S. solfataricus* Vps4 are disordered in the structure and indicated by a *dashed line*

contributing to the active site (Erzberger and Berger 2006). The predicted hexamer is ring-shaped with a central pore into which loops project (Fig. 12.4). By analogy with other AAA+ proteins, including the ClpX protein-unfoldase and DNA helicases, it is likely that these pore loops facilitate remodeling of Vps4's ESCRT-III substrate. Indeed, mutation of these loops impact upon Vps4's ability to function in human cells (Scott et al. 2005). Comparison of the structure of the AAA+ domain from Sso Vps4 with that of yeast Vps4p reveals a RMSD of 1.62 Å over 237 Cα atoms. The principal difference between the eukaryotic and archaeal structure lies in the absence or presence of a eukaryotic-specific 45-residue beta-strand-rich insertion in the smaller "lid" domain of the AAA+ module (green in Fig. 12.4). This serves as an interaction site for the eukaryotic-specific Vps4 activator protein Vta1 (Scott et al. 2005).

The N-terminal 75 residues of Vps4 form a three-helix bundle termed a MIT (**M**icrotubule **I**nteracting and **T**rafficking) domain. This domain is a versatile protein-protein interaction module that, as its name implies, has been identified in a number of proteins involved in cytoskeletal processes and trafficking, including katanin, spastin, Vps4 and Vta1 (Fig. 12.5). Studies in yeast and mammal systems revealed that the Vps4 MIT domain interacted with specific sequence motifs in

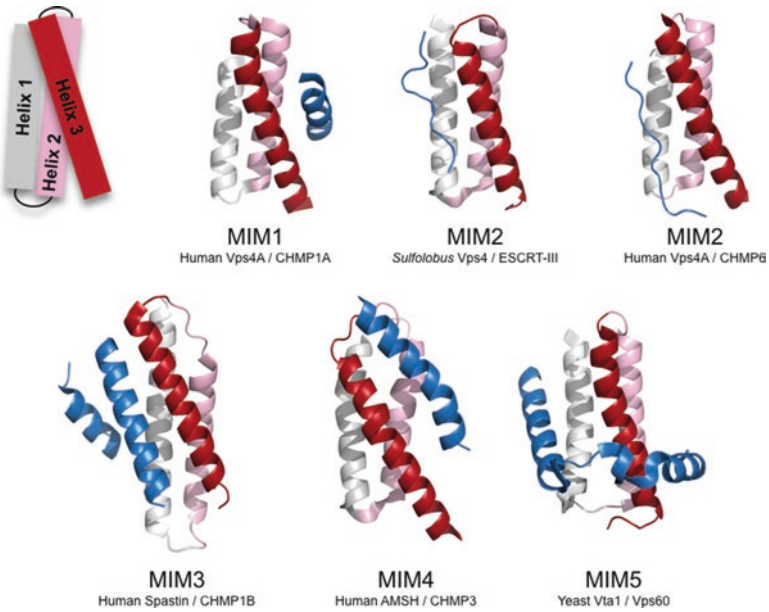

Fig. 12.5 Comparison of the structures of various MIT domains and their ESCRT-III interaction partners, demonstrating the distinct MIM1–5 binding modes. A schematic of the MIT domain is given in the *top left* and the color convention is adhered to in the subsequent images. The partner peptide is in blue. PDB codes are MIM1 – 2JQ9, *Sulfolobus* MIM2 – 2W2U, Human MIM2 – 2K3W, MIM3 – 3EAB, MIM4 – 2XZE and MIM5 – 2LUH. The CHMP and Vps60 proteins are all ESCRT-III family members

ESCRT-III proteins. Initial work identified a MIT-interacting motif (MIM) in yeast Vps2 and human CHMP1 and CHMP2B and revealed that they bound in the groove between the second and third helix of the MIT domain (Obita et al. 2007; Stuchell-Brereton et al. 2007). Subsequent work revealed that the human ESCRT-III protein CHMP6 also interacted with the MIT domain but, remarkably, utilized an alternate MIM, termed MIM2, that interacted with the groove between the first and third helix of the Vps4 MIT domain (Kieffer et al. 2008). More recently three additional modes of interaction between MIT domains and partner proteins have been described (MIM3–5; Fig. 12.5) (Yang et al. 2008, 2012; Solomons et al. 2011).

Interaction studies revealed that *Sulfolobus* Vps4 interacted specifically with the wH-containing ESCRT-III protein. The interaction interface was mapped to residues 183–193, between the core ESCRT-III fold and the C-terminal wH-like domain (Samson et al. 2008). The X-ray crystal structure of the ESCRT-III peptide•MIT domain complex revealed that the peptide from the ESCRT-III protein bound along the groove between helices 1 and 3 of the Vps4 MIT domain, utilizing the MIM2 mode of interaction (Fig. 12.5). Indeed, comparison of the archaeal and human MIM2•MIT domain interactions reveals clear conservation at the level of primary sequence (Samson et al. 2008; Kieffer et al. 2008). Thus, the ATPase Vps4 interacts with ESCRT-III subunits and ATP hydrolysis is required for Vps4 to fulfill its function. Recent work with yeast Vps4 and an artificial chimeric ESCRT-III substrate (Vps24–2) has revealed that Vps4 effects global unwinding of ESCRT-III while stripping protomers from a filament of the protein. In addition, the substrate passes through the central pore of the Vps4 during the unfolding reaction (Yang et al. 2015). While this mechanism has not yet been directly demonstrated for the archaeal proteins, given the conservation of the system and the demonstrated requirement for ATP hydrolysis by *Sufolobus* Vps4 for cell division, it seems likely that disassembly of the ESCRT-III structures seen at mid-cell will be similarly effected by Vps4.

As described above, there is currently no evidence for direct interactions of the archaeal ESCRT-III proteins with archaeal membranes. However, liposome-binding studies with Large Unilameller Vesicles (LUVs) reconstituted with purified *Sulfolobus* tetra-ether lipids revealed that the alpha-helical domain of CdvA bound directly to membranes (Samson et al. 2011). Like ESCRT-III, CdvA forms filaments, and negative stain electron microscopy provided evidence for a lattice-like structure forming on LUVs in the presence of CdvA. Strikingly, while ESCRT-III in isolation had no discernable effect on the LUVs, the addition of the wH-containing ESCRT-III to CdvA-coated LUVs resulted in dramatic deformation of the liposomes (Samson et al. 2011).

CdvA has a tri-partite structure with a ~ 70 residue beta-strand rich N-terminal domain, predicted to form a PRC barrel (Anantharaman and Aravind 2002), followed by an alpha-helix-rich region and finally a C-terminal domain that is poorly conserved in sequence apart from its final 10 amino-acids. The role of the PRC-domain remains undetermined, however, the alpha-helical region of the protein has been shown to interact with archaeal membranes. The C-terminal tail binds to the wH-like domain of the ESCRT-III paralog with a *Kd* of 6 μM. Further, disruption of this interaction *in vivo* leads to cell division defects (Samson et al. 2011).

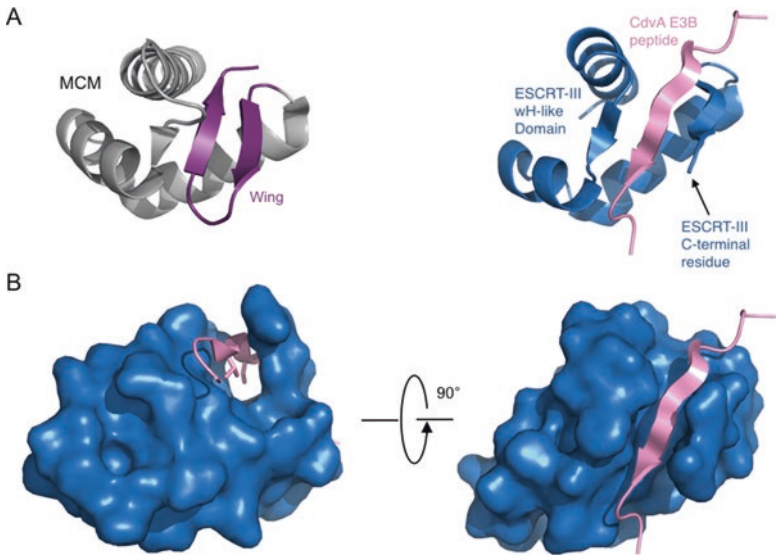

Fig. 12.6 (**a**) The *left*-hand image shows an example of the classical winged helix topology with the β-hairpin wing element highlighted in *purple*. The example shown is from *S. solfataricus* MCM (PDB 2 M45) in which this domain serves as a protein-protein interaction module (Samson et al. 2016; Wiedemann et al. 2015). The image on the *right* is the structure of the "broken wing" domain from the *S. solfataricus* ESCRT-III protein (*blue*) in complex with the E3B peptide from CdvA (*pink*), PDB 2XVC (Samson et al. 2011). (**b**) Two views, related by a 90° rotation, of a surface model of the ESCRT-III broken wing domain in complex with a cartoon view of the CdvA E3B peptide. The side-chains of two valine residues (V259 and V261) that important for the interaction are shown in stick mode in the left hand image

The crystal structure of the ESCRT-III-Binding (E3B) peptide of CdvA (residues 251–265) in complex with the wH-like domain of ESCRT-III (residues 210–259) was solved and revealed a novel mode of protein-protein interaction (Samson et al. 2011). Classical wH domains possess a three helix bundle surmounted by a pair of antiparallel β-strands that are connected by a turn of variable length (Fig. 12.6). This latter feature is the eponymous wing. Remarkably, the wH-like domain of the ESCRT-III protein is truncated, with the C-terminal residue of the protein at the end of the first of the β-strands, leaving a cleft in the surface of the protein. CdvA interacts with this cleft, in essence donating a β-strand to heal the broken wing structure. Hydrophobic residues, mutation of which impairs the interaction, dominate the inter-protein interface (Samson et al. 2011). A consequence of CdvA acting as a recruitment platform for ESCRT-III is that ESCRT-III could be spatially removed from the membrane by a distance equivalent to the depth of the CdvA lattice. As discussed below, this might have facilitated detection of the ESCRT-III membrane ingression belt by electron cryotomography (Dobro et al. 2013).

Ultrastructural Analyses of the Archaeal ESCRT Machinery

In 2013, we used electron cryotomography to explore the archaeal ESCRT machinery in *Sulfolobus* cells (Dobro et al. 2013). In electron cryotomography, samples are rapidly frozen, preserving them in a near-native, "frozen-hydrated" state. Samples are then imaged iteratively while being rotated around an axis to provide three-dimensional information. While each cryotomogram elucidates the structures present in a single moment, dynamic processes like cell division can be inferred by imaging different cells frozen at different stages of the process.

Previous images of purified eukaryotic ESCRT-III proteins had revealed that ESCRT-III proteins frequently polymerize into filaments, which then coil and spiral (Effantin et al. 2013). Adding to this body of information, we saw that purified CHMP1B, a human member of the ESCRT-III family, polymerized into helical filaments that formed 3-D bull's-eye patterns and stacked cones (Fig. 12.7). These assemblies contained layers of varying radii and angles, revealing that the lateral bonds between ESCRT filaments are non-specific, an essential property for spirals and coils. The stacked cones further revealed that ESCRT-III filaments were capable of binding each other on multiple surfaces including the top, sides, and bottom.

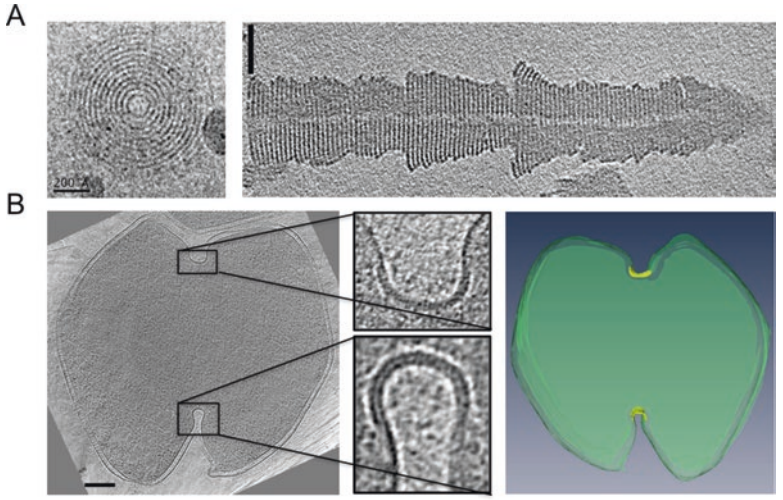

Fig. 12.7 (**a**) Electron microscopy projections of purified CHMP1B assemblies. The *left* hand image shows a view down the axis of a CHMP1B tube (scale bar 200 Å). The *right* hand image shows a central slice of a large CHMP1B assembly revealing layers of varying angles and radii. This implies that lateral bonds between filaments are non-specific and capable of binding on multiple surfaces, including the top, sides, and bottom. Scale bar is 500 Å. (**b**) A dividing *S. acidocaldarius* cell observed with electron cryotomography. The *left* hand images show a central slice of the tomogram with the division furrows magnified in the *offset* panels. The *right* hand image contains a model of that slice with the U-shaped protein coating on the division furrow colored in *yellow*. Scale bar is 200 nm (Figures adapted with permission from Dobro et al. 2013)

Moving to the archaeal proteins, we imaged mixtures of purified CdvA and liposomes made of *Sulfolobus* lipids. In this system, CdvA formed filaments of similar dimensions to ESCRT-III that wrapped around the liposomes. As described above, *Sulfolobus* ESCRT-III is recruited to membranes by CdvA. To observe these CdvA-ESCRT-III complexes in their physiological context, synchronized *Sulfolobus acidocaldarius* cells were collected at the time of division and rapidly frozen. Tomograms revealed that *every* cell displaying any membrane ingression also contained a thick, U-shaped protein belt around the constricting ring. The protein belt was also observed in cells with no visible constriction, indicating that the belt assembles before ingression begins (Dobro et al. 2013). This is unlike eukaryotic cells, which use ESCRT to divide only at the final scission stage when the diameter of the midbody site is approximately 100–200 nm (Elia et al. 2011; Agromayor and Martin-Serrano 2013).

By analogy to the properties of eukaryotic ESCRT-III's *in vitro* (Effantin et al. 2013; Dobro et al. 2013), the belts observed in dividing *Sulfolobus* cells were likely to be ESCRT-III filaments wrapped around the membrane in tight spirals. This is supported by comparing the dimensions of the belt to dimensions of known ESCRT crystal structures (Muziol et al. 2006; Bajorek et al. 2009). The belt appears dynamic in nature. During the process of constriction, the protein belt gets wider, yet the total surface area decreases. Importantly, the thickness remains the same. Together with all else that is known about the ESCRT machinery, this information supports a model we call the "hourglass" (Fig. 12.8). With mother and daughter cells stacked on top of each other, the protein belt around the middle forms an hourglass shape. This is similar to the proposed dome model for budding vesicles of eukaryotes, in which ESCRT-III forms dome-shaped spirals (Lata et al. 2008) but the symmetrical division septum forms two domes. In the hourglass model, two growing filaments (one on each side of the division plane) spiral towards each other into ever-smaller radii until the membranes are close enough for spontaneous scission (Video 12.1). While this hourglass model depends on ESCRT-III filaments being able to grow and bind each other along many surfaces as they progress from flat ribbons at the beginning to deeply invaginated U-shapes at the end, the *in vitro* assemblies demonstrate these capabilities.

The location and dimensions of the belt point to ESCRT-III as the candidate protein but, as discussed earlier, CdvA is likely linking ESCRT-III to the membrane (Samson et al. 2011). The belt was spaced about 6 nm from the membrane, which would accommodate CdvA as an adaptor (Fig. 12.8). As the membrane constrictions grew deeper in the various tomograms, the belt got wider but its total surface area decreased, suggesting Vps4 is actively re-modelling the ESCRT-III filaments during the process by removing ESCRT-III protomers. Since the diameter of the cytokinetic ring is decreasing toward zero, if the protein complexes were not being depleted, the late stage belt would have been extremely wide. Instead the belt only slightly increased in width, always at the leading edge of the division furrow.

Our images of dividing *Sulfolobus* cells do not support other models proposed in the literature These include the "purse-string" model in which Vps4 disassembles a ring filament by ESCRT-III protomer removal and resealing of the ring and the

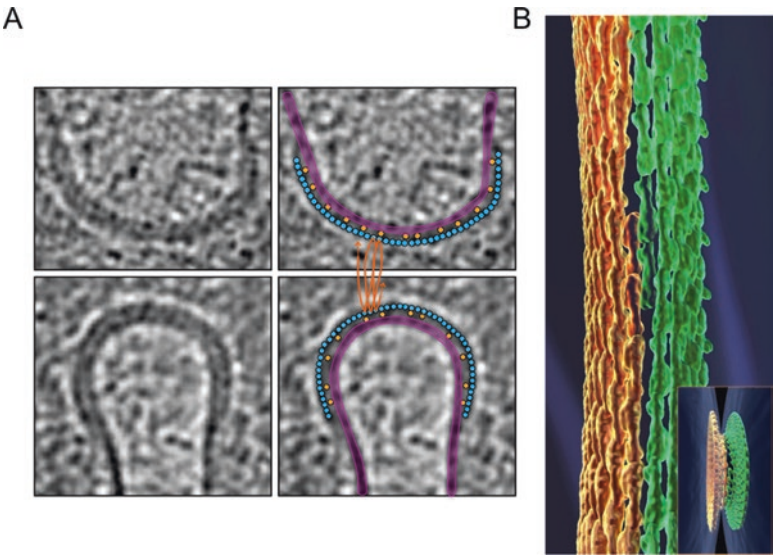

Fig. 12.8 (**a**) Interpretation of the protein belt as ESCRT helices. *Left* hand panels: central slices through opposing edges of the division furrow show the thick protein layer on the membrane. The *right* hand images show the same slices with the membrane (*purple*) and our model for how ESCRT (*blue*) filaments wrap helically (*orange lines*) around the cytokinetic ring to form the protein belt. The ESCRT filaments appear as *circles* because they are cut in cross section, but their diameter matches the width of the belt. CdvA filaments (*yellow*) link the membrane and ESCRT belt (Figures adapted with permission from Dobro et al. 2013). (**b**) Two spirals made of ESCRT monomers grow from the middle in opposite directions with a decreasing radius, pulling the membrane inward. The larger image is a close-up of the *inset* image

"whorl" model in which ESCRT-III filaments lie along the axis of a budding neck rather than spiraling around it (Saksena et al. 2009; Boura et al. 2012). Significantly, the data presented in the studies leading to those models also support the hourglass model. Filament growth in a spiraling pattern toward smaller radius may therefore drive constriction in cell division, as well as in vesicle and viral budding in eukaryotes.

Additional Roles for the Archaeal ESCRT Proteins

As described in the introduction, eukaryotic ESCRT proteins are involved in a broad range of membrane manipulation processes, both intrinsic to normal cellular metabolism but also imposed upon the cell by infectious agents (Hurley 2015). In regard to the latter, a number of enveloped viruses co-opt ESCRT proteins, including important pathogens such as HIV, Ebola, Hepatitis C, Rabies virus and Hepatitis B virus - see (Votteler and Sundquist 2013) for review. It has become apparent that there is a remarkable diversity of viruses infecting archaea (Prangishvili 2013), and

studies of one, ***S**ulfolobus* **T**urreted **I**cosahedral **V**irus (STIV) have implicated the archaeal ESCRT machinery as an important cellular facilitator of the viral life cycle (Snyder et al. 2013). STIV is a lytic virus and utilizes a remarkable mechanism of egress from infected cells (Brumfield et al. 2009). A single 92 amino acid viral gene product, C92, assembles seven-sided pyramid structures that project through the S-layer of the host cells. Eventually the facets of the pyramids separate from one another at the vertices, like petals opening in a flower, resulting in cell lysis and virus release. Remarkably, an otherwise completely unrelated rod-shaped *Sulfolobus* virus, also encodes a C92 ortholog and directs the assembly of analogous structures (Bize et al. 2009). No further viral proteins are required for pyramid assembly and it has been demonstrated that expression of the C92 ortholog in *E. coli* or budding yeast also results in formation of pyramids, although, intriguingly, those pyramids never open in these heterologous cells (Daum et al. 2014).

STIV virus particles assemble in the *Sulfolobus* cytosol. Initially, icosahedral particles assemble and package an internal host-derived lipid envelope structure. Subsequent embellishments to the capsids occur before viral genome packaging. Ultimately the mature virus particles are released through the open pyramid structures (Fu et al. 2010; Brumfield et al. 2009). The first hints of a role for the host ESCRT proteins in the STIV life cycle came from the observation that *Sulfolobus* ESCRT-III proteins were associated with purified viral particles. In addition, analyses of the host transcriptional reprograming upon viral infection revealed up-regulation of the ESCRT genes, including CdvA, ESCRT-III paralogs and Vps4 (Ortmann et al. 2008).

Protein-protein interaction studies have revealed an interaction between one ESCRT-III paralog (SSO0619) and the major capsid protein of STIV, termed B345. While the functional significance of this interaction has not been resolved, it is tempting to speculate that it may be indicative of a role for the ESCRT machinery in the maturation of the lipid envelope within the viral particle (Snyder et al. 2013). Additionally, an interaction between the C92 pyramid protein and the wH-containing and Vps4-interacting ESCRT-III protein was detected. Immunolocalization epifluorescence microscopy and electron microscopy coupled with immunogold staining revealed Vps4 recruitment to pyramid structures both in cells infected with STIV and cells expressing only the C92 protein from a plasmid. The importance of the integrity of the host ESCRT machinery for the viral life cycle was underscored by the observation that expression of the *trans*-dominant negative, ATP hydrolysis deficient, allele of Vps4 abrogated viral replication, while not impacting the ability of STIV to enter cells and execute viral gene expression (Snyder et al. 2013). While the molecular mechanisms of host ESCRT function in the STIV life-cycle remain to be resolved, it is possible that the ESCRT apparatus could act both at the level of initial particle assembly, conceivably in maturation of the inner capsid membrane, and possibly also at the level of viral egress (Snyder et al. 2013).

In contrast to the up-regulation of the ESCRT pathway in response to STIV infection, the host response to SIRV2 revealed down-regulation of the ESCRT apparatus (Okutan et al. 2013). More specifically, mRNA levels for CdvA, ESCRT-III and Vps4 were all reduced three- to ten-fold. As described above, SIRV2 also

utilizes the unusual pyramid structures to effect cell lysis. With regard to ESCRT functions in the viral life cycle, there are two potentially important differences between STIV and SIRV2. First, STIV has an internal membrane structure, SIRV2 does not. Second, the time course of infection is dramatically different for the two viruses. In the case of SIRV2 infection, pyramids appear between 6 and 9 h post-infection. This contrasts with STIV infection in which pyramids do not appear until 32 h post-infection. As SIRV2 infection leads to extensive host DNA degradation, it is possible that the down-regulation of ESCRT genes in response to SIRV2 could reflect a checkpoint-like response to inhibit cell division upon viral infection (Bize et al. 2009).

In addition to co-option by archaeal viruses, the *Sulfolobus* ESCRT apparatus may also play a role in the generation of extra-cellular vesicles. *Sulfolobus* cells secrete small vesicles during normal growth and in response to cellular stresses. Proteomic studies have demonstrated that these vesicles are associated with host ESCRT-III and Vps4 proteins (Ellen et al. 2009; Prangishvili et al. 2000). However, a causal linkage has yet to be established. As described above, a proteinaceous belt, presumed to be ESCRT-III, can be detected at mid-cell in dividing *Sulfolobus*. Intriguingly, the same tomograms reveal some cells extruding vesicles, yet examination of these structures does not provide evidence for an analogous belt-like feature at the vesicle necks (Dobro et al. 2013). Conceivably, the cell-division structure is discernable because of the role of CdvA as an adaptor between the membrane and ESCRT-III -assembly. If vesicle formation exploits a different adaptor protein, then an alternate morphology of the ESCRT-III at vesicle necks could exist. While this is complete speculation at this point, it is interesting to note that several of the *Thermococcales*, members of the euryarchaea, also produce extra-cellular vesicles and possess ESCRT-III and Vps4 homologs (Soler et al. 2008). However, they do not encode a detectable CdvA homolog and are thought to effect cell division using FtsZ (Fig. 12.2).

Future Directions

Our understanding of the biology of the archaeal ESCRT system remains very rudimentary at this time. While structural studies have illuminated the nature of the molecular handshakes that orchestrate assembly of the cytokinetic ring, how these events are appropriately coordinated in time and space remains largely unknown. The nature of the cell cycle oscillators that drive the regulated expression of the ESCRT genes is another key unresolved issue. Yet another lies in the coordinated assembly of CdvA at mid-cell. CdvA assembles prior to nucleoid segregation. Does CdvA, by polymerizing, define mid-cell and drive segregation away from its zone of assembly? Alternatively, are spatial cues established in the cell prior to CdvA assembly? What is the nature of the *Sulfolobus* DNA segregation machinery? Another utterly mysterious process lies in how S-layer assembly is coordinated with the division process. While key players in the assembly and glycosylation of S-layer

proteins have been identified, essentially nothing is known about how they are regulated and localized in the cell. The tomograms of dividing cells show a dramatic restructuring of the presumptive ESCRT-III belt, from a planar to a U-shaped topography. Is this due to a belt-intrinsic process, perhaps via differential incorporation of ESCRT-III paralogs, or is it mechanically driven by S-layer growth? It is anticipated that answers to many of these questions will be forthcoming over the next few years as advances in the genetic and cell biological analyses of archaea become ever more sophisticated.

References

Agromayor M, Martin-Serrano J (2013) Knowing when to but and run: mechanisms that control cytokinetic abscission. Trends Cell Biol 23:433–441

Anantharaman V, Aravind L (2002) The PRC-barrel: a widespread, conserved domain shared by photosynthetic reaction center subunits and proteins of RNA metabolism. Genome Biol 3**,** RESEARCH0061

Bajorek M, Schubert HL, Mccullough J, Langelier C, Eckert DM, Stubblefield WM, Uter NT, Myszka DG, Hill CP, Sundquist WI (2009) Structural basis for ESCRT-III protein autoinhibition. Nat Struct Mol Biol 16:754–762

Bang C, Schmitz RA (2015) Archaea associated with human surfaces: not to be underestimated. FEMS Microbiol Rev 39:631–648

Baumann P, Jackson SP (1996) An archaebacterial homologue of the essential eubacterial cell division protein FtsZ. Proc Natl Acad Sci U S A 93:6726–6730

Bernander R (1998) Archaea and the cell cycle. Mol Microbiol 29:955–961

Bize A, Karlsson EA, Ekefjard K, Quax TE, Pina M, Prevost MC, Forterre P, Tenaillon O, Bernander R, Prangishvili D (2009) A unique virus release mechanism in the Archaea. Proc Natl Acad Sci U S A 106:11306–11311

Boura E, Rozycki B, Chung HS, Herrick DZ, Canagarajah B, Cafiso DS, Eaton WA, Hummer G, Hurley JH (2012) Solution structure of the ESCRT-I and -II supercomplex: implications for membrane budding and scission. Structure 20:874–886

Breuert S, Allers T, Spohn G, Soppa J (2006) Regulated polyploidy in halophilic archaea. PLoS One:1

Brumfield SK, Ortmann AC, Ruigrok V, Suci P, Douglas T, Young MJ (2009) Particle assembly and ultrastructural features associated with replication of the lytic archaeal virus sulfolobus turreted icosahedral virus. J Virol 83:5964–5970

Carlton JG, Martin-Serrano J (2007) Parallels between cytokinesis and retroviral budding: A role for the ESCRT machinery. Science 316:1908–1912

Chen L, Brugger K, Skovgaard M, Redder P, She Q, Torarinsson E, Greve B, Awayez M, Zibat A, Klenk HP, Garrett RA (2005) The genome of Sulfolobus acidocaldarius, a model organism of the Crenarchaeota. J Bacteriol 187:4992–4999

Daum B, Quax TEF, Sachse M, Mills DJ, Reimann J, Yildiz O, Hader S, Saveanu C, Forterre P, Albers SV, kuhlbrandt W, Prangishvili D (2014) Self-assembly of the general membrane-remodeling protein PVAP into sevenfold virus-associated pyramids. Proc Natl Acad Sci U S A 111:3829–3834

Dobro MJ, Samson RY, Yu Z, Mccullough J, Ding HJ, Chong PL, Bell SD, Jensen GJ (2013) Electron cryotomography of ESCRT assemblies and dividing Sulfolobus cells suggests that spiraling filaments are involved in membrane scission. Mol Biol Cell 24:2319–2327

Dominguez-Escobar J, Chastanet A, Crevenna AH, Fromion V, Wedlich-Soldner R, Carballido-Lopez R (2011) Processive movement of MreB-associated cell wall biosynthetic complexes in bacteria. Science 333:225–228

Effantin G, Dordor A, Sandrin V, Martinelli N, Sundquist WI, Schoehn G, Weissenhorn W (2013) ESCRT-III CHMP2A and CHMP3 form variable helical polymers in vitro and act synergistically during HIV-1 budding. Cell Microbiol 15:213–226

Elia N, Sougrat R, Spurlin TA, Hurley JH, Lippincott-Schwartz J (2011) Dynamics of endosomal sorting complex required for transport (ESCRT) machinery during cytokinesis and its role in abscission. Proc Natl Acad Sci U S A 108:4846–4851

Ellen AF, Albers SV, Huibers W, Pitcher A, Hobel CFV, Schwarz H, Folea M, Schouten S, Boekema EJ, Poolman B, Driessen AJM (2009) Proteomic analysis of secreted membrane vesicles of archaeal Sulfolobus species reveals the presence of endosome sorting complex components. Extremophiles 13:67–79

Errington J (2015) Bacterial morphogenesis and the enigmatic MreB helix. Nat Rev Microbiol 13:241–248

Erzberger JP, Berger JM (2006) Evolutionary relationships and structural mechanisms of AAA plus proteins. Annu Rev Biophys Biomol Struct 35:93–114

Ettema TJ, Lindas AC, Bernander R (2011) An actin-based cytoskeleton in archaea. Mol Microbiol 80:1052–1061

Faguy DM, Doolittle WF (1999) Lessons from the Aeropyrum pernix genome. Curr Biol 9:R883–R886

Fitz-Gibbon ST, Ladner H, Kim UJ, Stetter KO, Simon MI, Miller JH (2002) Genome sequence of the hyperthermophilic crenarchaeon Pyrobaculum aerophilum. Proc Natl Acad Sci U S A 99:984–989

Frols S, Gordon PM, Panlilio MA, Duggin IG, Bell SD, Sensen CW, Schleper C (2007) Response of the hyperthermophilic archaeon Sulfolobus solfataricus to UV damage. J Bacteriol 189:8708–8718

Fu CY, Wang K, Gan L, Lanman J, Khayat R, Young MJ, Jensen GJ, Doerschuk PC, Johnson JE (2010) In vivo assembly of an archaeal virus studied with whole-cell electron cryotomography. Structure 18:1579–1586

Garner EC, Bernard R, Wang W, Zhuang X, Rudner DZ, Mitchison T (2011) Coupled, circumferential motions of the cell wall synthesis machinery and MreB filaments in *B. subtilis*. Science 333:222–225

Gotz D, Paytubi S, Munro S, Lundgren M, Bernander R, White MF (2007) Responses of hyperthermophilic crenarchaea to UV irradiation. Genome Biol 8:R220

Guy L, Ettema TJ (2011) The archaeal 'TACK' superphylum and the origin of eukaryotes. Trends Microbiol 19:580–587

Henne WM, Stenmark H, Emr SD (2013) Molecular mechanisms of the membrane sculpting ESCRT pathway. Cold Spring Harb Perspect Biol 5

Hurley JH (2015) ESCRTs are everywhere. EMBO J 34:2398–2407

Jones LJ, Carballido-Lopez R, Errington J (2001) Control of cell shape in bacteria: helical, actin-like filaments in Bacillus subtilis. Cell 104:913–922

Kawarabayasi Y, Hino Y, Horikawa H, Yamazaki S, Haikawa Y, Jin-No K, Takahashi M, Sekine M, Baba S, Ankai A, Kosugi H, Hosoyama A, Fukui S, Nagai Y, Nishijima K, Nakazawa H, Takamiya M, Masuda S, Funahashi T, Tanaka T, Kudoh Y, Yamazaki J, Kushida N, Oguchi A, Kikuchi H et al (1999) Complete genome sequence of an aerobic hyper-thermophilic crenarchaeon, Aeropyrum pernix K1. DNA Res 6(83–101):145–152

Kawarabayasi Y, Hino Y, Horikawa H, Jin-No K, Takahashi M, Sekine M, Baba S, Ankai A, Kosugi H, Hosoyama A, Fukui S, Nagai Y, Nishijima K, Otsuka R, Nakazawa H, Takamiya M, Kato Y, Yoshizawa T, Tanaka T, Kudoh Y, Yamazaki J, Kushida N, Oguchi A, Aoki K, Masuda S, Yanagii M, Nishimura M, Yamagishi A, Oshima T, Kikuchi H (2001) Complete genome sequence of an aerobic thermoacidophilic crenarchaeon, Sulfolobus tokodaii strain7. DNA Res 8:123–140

Kieffer C, Skalicky JJ, Morita E, De Domenico I, Ward DM, Kaplan J, Sundquist WI (2008) Two distinct modes of ESCRT-III recognition are required for VPS4 functions in lysosomal protein targeting and HIV-1 budding. Dev Cell 15:62–73

Lata S, Schoehn G, Jain A, Pires R, Piehler J, Gottlinger HG, Weissenhorn W (2008) Helical structures of ESCRT-III are disassembled by VPS4. Science 321:1354–1357
Lindas AC, Karlsson EA, Lindgren MT, Ettema TJG, Bernander R (2008) A unique cell division machinery in the Archaea. Proc Natl Acad Sci U S A 105:18942–18946
Lowe J, Amos LA (1998) Crystal structure of the bacterial cell-division protein FtsZ. Nature 391:203–206
Lundgren M, Malandrin L, Eriksson S, Huber H, Bernander R (2008) Cell cycle characteristics of Crenarchaeota: Unity among diversity. J Bacteriol 190:5362–5367
Maaty WS, Wiedenheft B, Tarlykov P, Schaff N, heinemann J, Robison-Cox J, Valenzuela J, Dougherty A, Blum P, Lawrence CM, Douglas T, Young MJ, Bothner B (2009) Something old, something new, something borrowed; how the thermoacidophilic archaeon Sulfolobus solfataricus responds to oxidative stress. PLoS One 4:e6964
Makarova KS, Yutin N, Bell SD, Koonin EV (2010) Evolution of diverse cell division and vesicle formation systems in Archaea. Nat Rev Microbiol 8:731–741
Margolin W, Wang R, Kumar M (1996) Isolation of an ftsZ homolog from the archaebacterium Halobacterium salinarium: implications for the evolution of FtsZ and tubulin. J Bacteriol 178:1320–1327
Mccullough J, Colf LA, Sundquist WI (2013) Membrane fission reactions of the mammalian ESCRT pathway. Annu Rev Biochem 82:663–692
Monroe N, Han H, Gonciarz MD, Eckert DM, Karren MA, Whitby FG, Sundquist WI, Hill CP (2014) The oligomeric state of the active Vps4 AAA ATPase. J Mol Biol 426:510–525
Morita E, Sandrin V, Chung HY, Morham SG, Gygi SP, Rodesch CK, Sundquist WI (2007) Human ESCRT and ALIX proteins interact with proteins of the midbody and function in cytokinesis. EMBO J 26:4215–4227
Muziol T, Pineda-Molina E, Ravelli RB, Zamborlini A, Usami Y, Gottlinger H, Weissenhorn W (2006) Structural basis for budding by the ESCRT-III factor CHMP3. Dev Cell 10:821–830
Obita T, Saksena S, Ghazi-Tabatabai S, Gill DJ, Perisic O, Emr SD, Williams RL (2007) Structural basis for selective recognition of ESCRT-III by the AAA ATPase Vps4. Nature 449:735–U11
Okutan E, Deng L, Mirlashari S, Uldahl K, Halim M, Liu C, Garrett RA, She QX, Peng X (2013) Novel insights into gene regulation of the rudivirus SIRV2 infecting Sulfolobus cells. RNA Biol 10:875–885
Ortmann AC, Brumfield SK, Walther J, Mcinnerney K, Brouns SJJ, Van De Werken HJG, Bothner B, Douglas T, Van De Oost J, Young MJ (2008) Transcriptome analysis of infection of the Archaeon Sulfolobus solfataricus with Sulfolobus turreted icosahedral virus. J Virol 82:4874–4883
Prangishvili D (2013) The wonderful world of archaeal viruses. Annu Rev Microbiol 67:565–585
Prangishvili D, Holz I, Stieger E, Nickell S, Kristjansson JK, Zillig W (2000) Sulfolobicins, specific proteinaceous toxins produced by strains of the extremely thermophilic archaeal genus Sulfolobus. J Bacteriol 182:2985–2988
Preston CM, Wu KY, Molinski TF, Delong EF (1996) A psychrophilic crenarchaeon inhabits a marine sponge: Cenarchaeum symbiosum gen. nov., sp. nov. Proc Natl Acad Sci U S A 93:6241–6246
Rivera MC, Lake JA (2004) The ring of life provides evidence for a genome fusion origin of eukaryotes. Nature 431:152–155
Robinson NP, Blood KA, Mccallum SA, Edwards PAW, Bell SD (2007) Sister chromatid junctions in the hyperthermophilic archaeon Sulfolobus solfataricus. EMBO J 26:816–824
Saksena S, Wahlman J, Teis D, Johnson AE, Emr SD (2009) Functional reconstitution of ESCRT-III assembly and disassembly. Cell 136:97–109
Samson RY, Bell SD (2011) Cell cycles and cell division in the archaea. Curr Opin Microbiol 14:350–356
Samson RY, Bell SD (2014) Archaeal chromosome biology. J Mol Microbiol Biotechnol 24:420–427
Samson RY, Obita T, Freund SM, Williams RL, Bell SD (2008) A Role for the ESCRT System in Cell Division in Archaea. Science 322:1710–1713

Samson RY, Obita T, Hodgson B, Shaw MK, Chong PL, Williams RL, Bell SD (2011) Molecular and structural basis of ESCRT-III recruitment to membranes during archaeal cell division. Mol Cell 41:186–196

Samson RY, Abeyrathne PD, Bell SD (2016) Mechanism of archaeal MCM helicase recruitment to DNA replication origins. Mol Cell 61:287–296

Schink B (1997) Energetics of syntrophic cooperation in methanogenic degradation. Microbiol Mol Biol Rev 61:262–280

Scott A, Chung HY, Gonciarz-Swiatek M, Hill GC, Whitby FG, Gaspar J, Holton JM, Viswanathan R, Ghaffarian S, Hill CP, Sundquist WI (2005) Structural and mechanistic studies of VPS4 proteins. EMBO J 24:3658–3669

She Q, Singh RK, Confalonieri F, Zivanovic Y, Allard G, Awayez MJ, Chan-Weiher CCY, Clausen IG, Curtis BA, De Moors A, Erauso G, Fletcher C, Gordon PMK, Heikamp-De Jong I, Jeffries AC, Kozera CJ, Medina N, Peng X, Thi-Ngoc HP, Redder P, Schenk ME, Theriault C, Tolstrup N, Charlebois RL, Doolittle WF, Duguet M, Gaasterland T, Garrett RA, Ragan MA, Sensen CW, Van Der Oost J (2001) The complete genome of the crenarchaeon Sulfolobus solfataricus P2. Proc Natl Acad Sci U S A 98:7835–7840

Snyder JC, Samson RY, Brumfield SK, Bell SD, Young MJ (2013) Functional interplay between a virus and the ESCRT machinery in archaea. Proc Natl Acad Sci U S A 110:10783–10787

Soler N, Marguet E, Verbavatz JM, Forterre P (2008) Virus-like vesicles and extracellular DNA produced by hyperthermophilic archaea of the order Thermococcales. Res Microbiol 159:390–399

Solomons J, Sabin C, Poudevigne E, Usami Y, Hulsik DL, Macheboeuf P, Hartlieb B, Gottlinger H, Weissenhorn W (2011) Structural basis for ESCRT-III CHMP3 recruitment of AMSH. Structure 19:1149–1159

Spang A, Saw JH, Jorgensen SL, Zaremba-Niedzwiedzka K, Martijn J, Lind AE, Van Eijk R, Schleper C, Guy L, Ettema TJG (2015) Complex archaea that bridge the gap between prokaryotes and eukaryotes. Nature 521:173–179

Stahl DA, De La Torre JR (2012) Physiology and diversity of ammonia-oxidizing archaea. Annu Rev Microbiol 66:83–101

Stuchell-Brereton MD, Skalicky JJ, Kieffer C, Karren MA, Ghaffarian S, Sundquist WI (2007) ESCRT-III recognition by VPS4 ATPases. Nature 449:740–744

Swulius MT, Jensen GJ (2012) The helical MreB cytoskeleton in *Escherichia coli* MC1000/pLE7 is an artifact of the N-Terminal yellow fluorescent protein tag. J Bacteriol 194:6382–6386

Votteler J, Sundquist WI (2013) Virus budding and the ESCRT pathway. Cell Host Microbe 14:232–241

Wang X, Lutkenhaus J (1996) FtsZ ring: the eubacterial division apparatus conserved in archaebacteria. Mol Microbiol 21:313–319

Wiedemann C, Szambowska A, Hafner S, Ohlenschlager O, Guhrs KH, Gorlach M (2015) Structure and regulatory role of the C-terminal winged helix domain of the archaeal minichromosome maintenance complex. Nucleic Acids Res 43:2958–2967

Williams TA, Foster PG, Cox CJ, Embley TM (2013) An archaeal origin of eukaryotes supports only two primary domains of life. Nature 504:231–236

Woese CR, Fox GE (1977) Phylogenetic structure of the prokaryotic domain: the primary kingdoms. Proc Natl Acad Sci U S A 74:5088–5090

Wollert T, Hurley JH (2010) Molecular mechanism of multivesicular body biogenesis by ESCRT complexes. Nature 464:864–U73

Wurtzel O, Sapra R, Chen F, Zhu YW, Simmons BA, Sorek R (2010) A single-base resolution map of an archaeal transcriptome. Genome Res 20:133–141

Yang N, Driessen AJ (2014) Deletion of cdvB paralogous genes of Sulfolobus acidocaldarius impairs cell division. Extremophiles 18:331–339

Yang D, Rismanchi N, Renvoise B, Lippincott-Schwartz J, Blackstone C, Hurley JH (2008) Structural basis for midbody targeting of spastin by the ESCRT-III protein CHMP1B. Nat Struct Mol Biol 15:1278–1286

Yang Z, Vild C, Ju J, Zhang X, Liu J, Shen J, Zhao B, Lan W, Gong F, Liu M, Cao C, Xu Z (2012) Structural basis of molecular recognition between ESCRT-III-like protein Vps60 and AAA-ATPase regulator Vta1 in the multivesicular body pathway. J Biol Chem 287:43899–43908

Yang B, Stjepanovic G, Shen Q, Martin A, Hurley JH (2015) Vps4 disassembles an ESCRT-III filament by global unfolding and processive translocation. Nat Struct Mol Biol 22:492–498

Yutin N, Wolf MY, Wolf YI, Koonin EV (2009) The origins of phagocytosis and eukaryogenesis. Biol Direct 4:9

Zerulla K, Soppa J (2014) Polyploidy in haloarchaea: advantages for growth and survival. Front Microbiol 5:274